tvst

Article

Deep Learning for Anterior Segment Optical Coherence Tomography to Predict the Presence of Plateau Iris

Boonsong Wanichwecharungruang[1], Natsuda Kaothanthong[2], Warisara Pattanapongpaiboon[1], Pantid Chantangphol[2], Kasem Seresirikachorn[1], Chaniya Srisuwanporn[1,3], Nucharee Parivisutt[1], Andrzej Grzybowski[4,5], Thanaruk Theeramunkong[2], and Paisan Ruamviboonsuk[1]

[1] Department of Ophthalmology, Rajavithi Hospital, Bangkok, Thailand
[2] Sirindhorn International Institute of Technology, Thammasat University, Pathumthani, Thailand
[3] Department of Ophthalmology, Panyananthaphikkhu Chonprathan Hospital, Nonthaburi, Thailand
[4] Department of Ophthalmology, University of Warmia and Mazury, Olsztyn, Poland
[5] Institute for Research in Ophthalmology, Poznan, Poland

Correspondence: Natsuda Kaothanthong, Sirindhorn International Institute of Technology, Thammasat University, 131 Moo5, Tiwanont Road, Bangkadi, Muang, Pathumthani 12000, Thailand.
e-mail: natsuda@siit.tu.ac.th

Received: August 13, 2020
Accepted: December 10, 2020
Published: January 6, 2021

Keywords: plateau iris; primary angle-closure glaucoma; ultrasound biomicroscopy; anterior segment optical coherence tomography (AS-OCT); Asian; diagnostic performance; sensitivity; specificity; accuracy; ocular imaging; deep learning (DL); style transfer; artificial intelligence

Citation: Wanichwecharungruang B, Kaothanthong N, Pattanapongpaiboon W, Chantangphol P, Seresirikachorn K, Srisuwanporn C, Parivisutt N, Grzybowski A, Theeramunkong T, Ruamviboonsuk P. Deep learning for anterior segment optical coherence tomography to predict the presence of plateau iris. Trans Vis Sci Tech. 2021;10(1):7, https://doi.org/10.1167/tvst.10.1.7

Purpose: The purpose of this study was to evaluate the diagnostic performance of deep learning (DL) anterior segment optical coherence tomography (AS-OCT) as a plateau iris prediction model.

Design: We used a cross-sectional study of the development and validation of the DL system.

Methods: We conducted a collaboration between a referral eye center and an informative technology department. The study enrolled 179 eyes from 142 patients with primary angle closure disease (PACD). All patients had remaining appositional angle after iridotomy. Each eye was scanned in four quadrants for both AS-OCT and ultrasound biomicroscopy (UBM). A DL algorithm for plateau iris prediction of AS-OCT was developed from training datasets and was validated in test sets. Sensitivity, specificity, and area under the receiver operating characteristics curve (AUC-ROC) of the DL for predicting plateau iris were evaluated, using UBM as a reference standard.

Results: Total paired images of AS-OCT and UBM were from 716 quadrants. Plateau iris was observed with UBM in 276 (38.5%) quadrants. Trainings dataset with data augmentation were used to develop an algorithm from 2500 images, and the test set was validated from 160 images. AUC-ROC was 0.95 (95% confidence interval [CI] = 0.91 to 0.99), sensitivity was 87.9%, and specificity was 97.6%.

Conclusions: DL revealed a high performance in predicting plateau iris on the noncontact AS-OCT images.

Translational Relevance: This work could potentially assist clinicians in more practically detecting this nonpupillary block mechanism of PACD.

Introduction

Plateau iris is a configuration of peripheral iris, a mechanism which can be attributable to nonpupillary block of angle closure in primary angle-closure disease (PACD).[1] The pathophysiology of angle closure in plateau iris is related to an anteriorly positioned ciliary process, leading to a posterior-pushing mechanism in PACD.[1] This nonpupillary block mechanism may not be able to be successfully treated with conventional laser peripheral iridotomy (LPI); however, laser iridoplasty, with the aim of modifying the configuration of peripheral iris, may be indicated to prevent permanent angle closure in this condition. It is, therefore, important to rule out plateau iris in eyes with PACD.

The standard method of detecting plateau iris can be based on either dynamic gonioscopy[2] or ultrasound biomicroscopy (UBM).[3] The former is a subjective examination, which requires examiner skills and expertise, whereas the latter is an objective investigation for direct imaging of angle structures behind the iris. UBM has been the preferred method for detecting plateau iris in recent studies, as the crucial findings for the determination of plateau iris include the anterior ciliary position, the absence of ciliary sulcus, and iris root angulation, which can be better visualized using UBM.[4,5] There are limitations, however, in applying UBM in routine clinical practice because it requires a contact immersion scanning technique under skilled operators.

Anterior segment optical coherence tomography (AS-OCT), a recently developed imaging technology, has been used for PACD evaluation in various situations. Without contacting ocular structures, AS-OCT applies a 1310-nm diode laser to visualize anterior segment structures, such as the cornea, iris, and anterior chamber angle.[6] It facilitates clinicians for the qualitative and quantitative evaluation of the anterior segment structures in more practical ways in comparison to UBM.[7] The diode laser, however, poorly penetrates the iris pigment epithelium; thus, it is unable to visualize the ciliary process and ciliary sulcus. Unlike UBM, indirect signs of the peripheral iris configuration are required for detection of plateau iris from AS-OCT.[8]

Deep learning (DL) is a subfield of machine learning in artificial intelligence. It uses several artificial neural network layers to learn patterns of existing data to generate a set of knowledge and then applies it to infer predictions from new data. With recent increased computing power and big data, DL has shown very promising diagnostic performance in medical imaging analysis[9,10] as well as in classification tasks in ophthalmology.[9–16] Interestingly, some DL models have been tentatively used for the classification or prediction of disease across two diverse types of information or imaging modalities; for example, the DL models have been trained to predict the presence or absence of glaucoma based on retinal nerve fiber layer (RNFL) thickness at the optic nerve head (ONH) on OCT from the grading on color photographs of the ONH. The predictions from this grading have been found to be on a par with the detection from actual measurement of RNFL thickness.[17]

In this study, we developed a DL model that would be capable of detecting plateau iris from AS-OCT images using data from paired images from UBM and AS-OCT for training, and UBM images as ground truth for validation. To further improve model performance, another unsupervised DL approach of image-to-image translation from UBM to AS-OCT was also conducted. This model could have an advantage due to the more practical, noncontact imaging modality of AS-OCT, and could potentially provide more accurate outcomes in predicting the presence of plateau iris on the same level of the contact imaging modality of UBM.

Patients and Methods

This study was a collaboration among the Department of Ophthalmology, Rajavithi Hospital, and Sirindhorn International Institute of Technology (SIIT), Thammasat University. The study protocol was approved by the institutional review boards of both institutes, informed consent was read and signed by all participants, and all images were de-identified for patient confidentiality. From March 2019 to January 2020, patients in the Glaucoma Clinic of Rajavithi Hospital with PACD, including primary angle-closure suspect (PACS), primary angle-closure (PAC), and primary angle-closure glaucoma (PACG), were enrolled into the study. The definition of the three diagnoses of PACD were based on the classification by Foster et al.[18]

Complete ocular examinations were performed in all patients using slit lamps, Goldman applanation tonometry, gonioscopy, visual field test, and ONH evaluation, and axial length was obtained using IOL Master (Carl Zeiss Meditec, Dublin, CA). Paired sets of scans from AS-OCT and UBM on the same day of examination were obtained for each of the enrolled participants. All patients had phakic eyes when the paired scans were obtained, and LPI was performed to

eliminate pupillary block in all eyes at least 1 month before the scans.

For AS-OCT, the patients were scanned in a sitting position using Visante (Model 1000, version 3.0.1.8; Carl Zeiss Meditec) for both horizontal and vertical axes. For UBM, the scans were conducted by our trained doctors (C.S. and W.W.) on superior, inferior, nasal, and temporal angles using an immersion technique with patients in a supine position. We used two UBM devices in this study: P60 (Paradigm Medical Industries Inc., Salt Lake City, UT) for the first 78 patients, and VuMAX HD (Sonomed Escalon, Lake Success, NY) for the other 64 patients. The procedures were performed in the same standard room light for the two devices. The AS-OCT images from the vertical and horizontal axes were then split into images from the superior, inferior, nasal, and temporal quadrants to match the corresponding images of each quadrant from UBM.

Patients were excluded from the study if they were undergoing treatment with pilocarpine, had a history of laser iridoplasty, glaucoma surgery (trabeculectomy, glaucoma tube shunt, or goniosynechialysis), opaque cornea, nanophthalmos, iridociliary cyst, or other ocular conditions that could not be applied to both AS-OCT and UBM investigations.

Classification of Plateau Iris Using UBM Criteria

Classification of the presence or absence of plateau iris was made for each quadrant image from UBM according to standard protocol.[19] Its presence was labeled when an anteriorly positioned ciliary process, obliteration of the ciliary sulcus, iris root angulation, and narrow anterior chamber angle were found. The images of quadrants without any of these signs were labeled as absence. These labels, determined by a senior glaucoma specialist (B.W.), were used as the reference standard, and intra-observer agreement was assessed for reproducibility of the classification on 30 images, kappa = 0.79. Interobserver agreements were tested by two glaucoma specialists (N.P. and K.S.), kappa = 0.73 and 0.71, respectively.

Prediction of Presence or Absence of Plateau Iris With AS-OCT Using a Deep Learning Model

We applied DL architecture, ResNet, for prediction of the presence or absence of plateau iris from AS-OCT images. To achieve an appropriate image dataset size, a pretraining model and image augmentation were applied. The Pre-trained Unsupervised Network (PUN) comprises a family of DL models that use unsupervised learning to train each hidden layer within a neural network in order to achieve a more accurate fitting of the dataset.[20] Data augmentation was performed to increase the data size and variation. With augmentation, the prediction model should be more generalized and invariant to certain types of data or images; in this study, four image augmentation methods were applied.

Original images were augmented using four transformation functions: flipping, rotation, contrast enhancement, and intensity adjustment. The flipping function reversed the pixels of the image in horizontal position, akin to a mirror effect, and the rotation function turned the image with a set of specified degrees. The contrast enhancement exaggerated the visible difference between the two adjacent structures, for example, the edge, in order to emphasize its details. The intensity adjustment mapped values of the intensity of an image into a new range for the purpose of brightness increment or decrement.

In addition to these transformations, we designed a process to utilize the UBM images in order to enhance the AS-OCT ones with a DL-based algorithm, namely style transfer,[21] an unsupervised DL-based approach (Cycle Generative Adversarial Network or CycleGAN) that performs image-to-image translation. Given two domains of images, it produces a new one by combining the content of one image domain with the style of the other. In addition, it can also map the content between the two image collections.[22] In this study, a style transfer of paired images (i.e. AS-OCT and UBM), was applied in a way that an AS-OCT image was considered as an image's content, whereas the corresponding UBM image was a style. Examples of the images with style transfer are shown in Supplementary Figure S1. They were the outcomes of mapping the style of UBM taken from the same quadrant of the same eye of a patient into the content of AS-OCT. With the features of the peripheral iris transferred and combined from the corresponding UBM images, together with the labels of the original images, and some with other augmentation functions also transferred from UBM, the knowledge from UBM images could be learned by the ResNet DL model in order to make a prediction about the presence or absence of plateau iris on AS-OCT images.

Data Collection and Preparation

We collected images from 179 eyes of 142 Asian patients, 109 (76.8%) of whom were women. There were 716 images of scanned quadrants of these eyes for

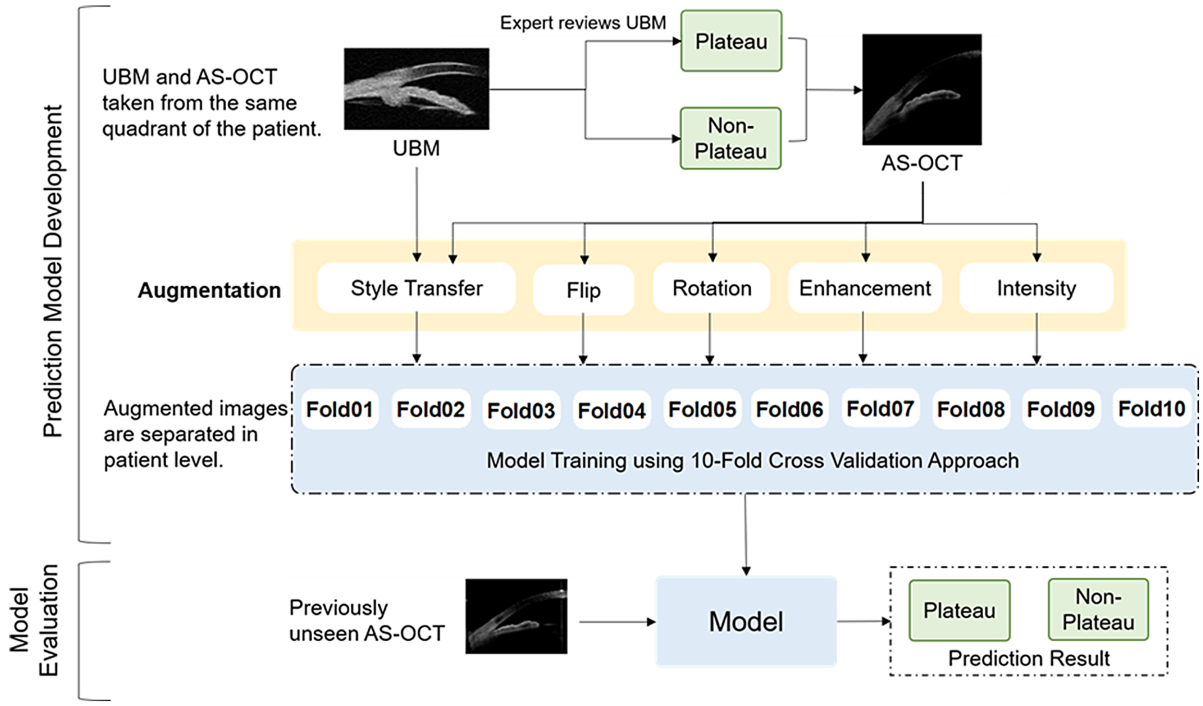

Figure 1. Overview of the proposed method.

both AS-OCT and UBM. Of the 716 AS-OCT images of 179 eyes, images of 139 eyes (77.7%) were randomly selected for training and those of the other 40 (22.3%) were used for testing the model.

From the original 218 images of quadrants with the presence of plateau iris (P) and 338 with the absence of plateau iris (NP), 1200 and 1300 augmented images, respectively, were constructed in order to balance the number of images with P and NP in the training dataset. The number of images from each function of augmentation was determined taking into consideration the quality of the original image and the necessity of the reconstruction. Examples of the augmented images and the number of images in each augmentation function are shown in Supplementary Figure S2.

The augmented AS-OCT images taken from each patient were labeled according to the reference standard labels determined from UBM images and assigned to the original AS-OCT ones. The patients were divided into 10 groups, each comprising 7 to 8 patients, and the AS-OCT images of these groups were used for training the model. The total number of images in the training dataset was 2500.

Training and Testing the Model

The 50-layered ResNet architecture (ResNet50) was applied with the pretraining model to assign an initial weight. For each training iteration, the images were trained with a batch size of 32, with 50 epochs (iterations), and the best learning rate, which was found using the cyclical learning method with stochastic gradient descent with restarts.

The performance of the model was measured using a 10-fold cross validation. As stated previously, the patients were independently classified into 10 groups; each group is considered a fold. Because the folds were classified on a patient level, the images that were augmented from the four quadrants of the same patient and eye were included in the same fold. For each round of training, nine groups of patients were used as a training set, and the others were used as a test set (see Fig. 1). The total number of rounds for training the model is 10. Among 10-fold cross validation, the model that achieved the highest accuracy was selected and tested using a test set. The AS-OCT images taken from the 4 quadrants of the 40 eyes, which had not been used in the training set, were used as a test set. There were in total 160 images of quadrants; 58 were labelled as P, and 102 as NP according to the reference standard in the test set. To test the model, each AS-OCT image alone without UBM was directly supplied to the model for prediction.

Statistics

Sensitivity, specificity, and accuracy were used as measurements of model performance. To visualize the

Table 1. Demographic Data from Primary Angle-Closure Disease

Patient-Wise	Total ($N = 142$ Patients)	Training Set ($N = 118$ Patients)	Testing Set ($N = 38$ Patients)
Mean age, y	62.45 ± 8.50	62.29 ± 8.69	63.45 ± 7.84
Range	42-87	42-87	49-79
Sex:			
Female, *N* eye	109 (76.80%)	88 (74.60%)	32 (84.20%)
Eye-wise	**Total (N = 179 eyes)**	**Training set (N = 139 eyes)**	**Testing set (N = 40 eyes)**
Diagnosis, *N*			
PACS	52 (29.1%)	45 (32.4%)	7 (17.5%)
PAC	33 (18.4%)	25 (18.0%)	8 (20.0%)
PACG	94 (52.5%)	69 (49.6%)	25 (62.5%)
VA, logMAR:			
Mean ± SD	0.35 ± 0.51	0.34 ± 0.49	0.37 ± 0.58
Median	0.20 (0.10, 0.40)	0.20 (0.10, 0.40)	0.20 (0.18, 0.38)
IOP mm Hg ± SD	17.0 ± 7.21	16.91 ± 7.43	17.31 ± 6.42
Range	8–56	8–56	10–44
Cup to disc ratio	0.54 ± 0.20	0.53 ± 0.20	0.62 ± 0.19
Range	0.2–0.9	0.2–0.9	0.3–0.9
Axial length, mm	22.59 ± 1.03	22.58 ± 0.99	22.63 ± 1.19
Range	19.07–27.88	19.14–27.88	19.07–27.69
Plateau iris			
Inferior quadrant	58 (32.40%)	47 (33.8%)	11 (27.5%)
Nasal quadrant	58 (32.40%)	45 (32.4%)	13 (32.5%)
Superior quadrant	69 (38.55%)	55 (39.6%)	14 (35.0%
Temporal quadrant	91 (50.84%)	71 (51.1%)	20 (50.0%)
Image-wise	**Total (*N* = 716 images)**	**Training set before augmentation (*N* = 556 images)**	**Testing set (*N* = 160 images)**

performance in distinguishing between the presence and absence of plateau iris, a receiver operation characteristic (ROC) and area under curve (AUC) were also depicted.

The prediction result obtained from each fold was computed. The probabilities of each augmented image derived from the same original input image were averaged to generate a final image-wise prediction of an original image. It was predicted as positive (plateau iris) if the probability was greater than or equal to 0.5; otherwise, it was predicted as negative.

Results

Demographic data of the patients are shown in Table 1. The proportions of patients and eyes in each of the parameters, including each of the PACD categories, were randomly distributed in training and test sets as shown. Plateau iris was found in 276 quadrants (38.55%) with the highest prevalence in the temporal quadrant ($N = 91$, 32.97%). A total of 85 from 179 eyes (47.49%) had at least 2 quadrants of plateau iris.

Training Results

From the 10-fold cross validation experiment in the training dataset, the DL prediction model achieved 96.50% sensitivity, 98.90% specificity, and 97.90% accuracy. It incorrectly predicted seven positive images of plateau iris as negative, whereas three negative images were incorrectly predicted as positive.

A comparison of the prediction result of each augmentation function is shown in the form of ROC curves in Supplementary Figure S3a. The prediction probability of each original image of the same augmentation function was averaged for a positive or negative prediction, and the final prediction was from the class that achieved a higher average probability. The

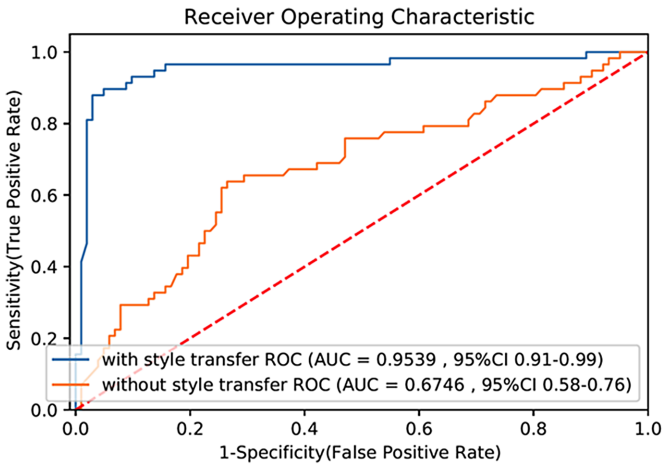

Figure 2. A comparison of ROC-AUC of the test set applying the style transfer augmentation for model training and the one without it.

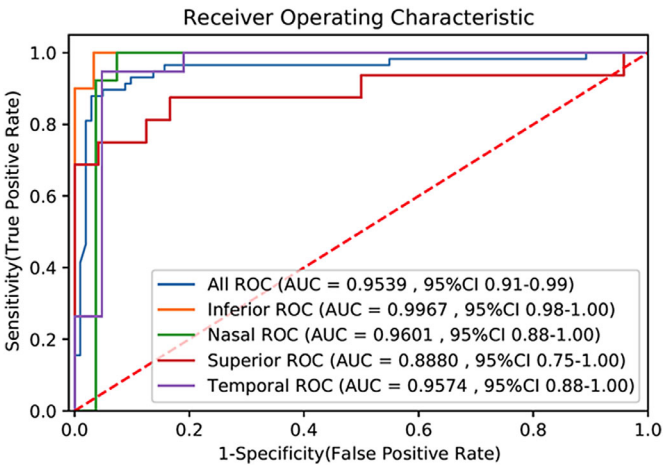

Figure 3. A comparison of ROC-AUC curve of the four quadrants in the test set of the prediction model with style transfer augmentation.

result showed that the AUC from each augmentation function was in a narrow range with the highest AUC from an enhanced function that achieved 0.9865 (95% confidence interval [CI] = 0.97 to 0.99). The lowest AUC was from style transfer at 0.9661 (95% CI = 0.95 to 0.98).

Training With and Without Style Transfer

We also trained another prediction model using 2500 augmented images with the same setting described previously for training, but all the DL-based style transfer images were replaced randomly with some from the other 4 augmentation functions. The ROC curve of the prediction result of each augmentation function in training is shown in Supplementary Figure S3b. Without the style transfer, the prediction result was less than the lowest AUC of the model with the style transfer as shown in Supplementary Figure S3a, which was 0.9661.

Testing Results

The sensitivity of the DL model for predicting plateau iris on AS-OCT images in the test set was 87.93%, the specificity was 97.06%, and the accuracy was 93.75 %. Out of 58 positive images of plateau iris, the model correctly detected 51 images, and it correctly detected 99 out of 102 negative images.

The AUC was 0.9539 (95% CI = 0.91 to 0.99) with the ROC-AUC curve shown in Figure 2. A comparison of the ROC-AUC curves of models with and without style transfer in the test set is shown in Figure 2. The AUC of the model with style transfer was 0.95 (95% CI = 0.91 to 0.99), whereas that of the model without style transfer was 0.67 (95% CI = 0.58 to 0.76).

A comparison of the sensitivity, specificity, and accuracy of the model for predicting plateau iris in each quadrant is shown in Table 2. The temporal quadrant achieved the highest sensitivity of 94.74%, and the inferior quadrant achieved the highest specificity of 100%. The superior quadrant achieved the lowest sensitivity of 75%, whereas the temporal quadrant achieved the lowest specificity of 95.24%. A comparison of ROC-AUC curves from the prediction of plateau iris in each quadrant is displayed in Figure 3.

At patient level, for those who had plateau iris in at least 2 quadrants (85 eyes), sensitivity was 83.3%, specificity was 95.5%, and accuracy was 90%. Examples of AS-OCT images that achieved the highest prediction scores are shown in Supplementary Figures S4(a) and S4(b) for the presence and absence respectively of plateau iris. Examples of images with the lowest prediction scores for false positive and predictions are shown in Supplementary Figures S5(a) and S5(b) respectively. The high-intensity pixels in the heatmap images in Supplementary Figures S4 and S5 show the locations of the model used for the prediction. The most common locations were the anterior chamber angle and adjacent structures. Comparing the images with the highest and lowest prediction scores, these high-intensity pixels were located closely in a similar location (the angle areas) in the former, whereas the pixels were dispersed in different locations in the latter.

Discussion

In the present study, DL of AS-OCT achieved high accuracy of plateau iris prediction. Sensitivity

Table 2. Comparison of Sensitivity, Specificity, Accuracy, and AUC of the Model with Style Transfer for Predicting Plateau Iris in Each Quadrant in the Test Set

	Inferior Quadrant $n = 40$	Nasal Quadrant $n = 40$	Superior Quadrant $n = 40$	Temporal Quadrant $n = 40$	Total $n = 160$
Sensitivity	90%	92.31%	75%	94.74%	87.93%
Specificity	100%	96.30%	95.83%	95.24%	97.06%
Positive predictive value	100%	92.31%	92.31%	94.74%	94.44%
Negative predictive value	96.77%	96.30%	85.19%	95.24%	93.40%
Accuracy	97.50%	95%	87.50%	95%	93.75%
AUC (95% CI)	0.99 (0.98–1.00)	0.96 (0.88–1.00)	0.88 (0.75–1.00)	0.95 (0.88–1.00)	0.95 (0.91–0.99)

and specificity showed good diagnostic performance to classify the disease. Previous studies have demonstrated the potential of using DL to classify angle-closure and open-angle from AS-OCT images with high accuracy when gradings of either AS-OCT images or gonioscopy were the reference standard.[23,24]

In a study by Fu et al.,[23] approximately 8200 anterior chamber angle (ACA) images of AS-OCT, 10% of which were angle-closure and 90% open-angle, were used for development of a DL model (VGG-16 architecture with additional techniques of transfer learning and data augmentation) to detect the presence of angle-closure. This study achieved a sensitivity of 0.90, a specificity of 0.92, and AUC of 0.96; however, there was no validation in the test set in this study.

In another study by Xu et al.,[24] approximately 4000 AS-OCT images were assigned as a test set and 3400 images as a cross-validation set with about half open-angle and the other half angle-closure in each of the datasets. A ResNet-18 classifier was able to detect gonioscopic angle-closure in the test set with an AUC of 0.93.

There has not yet been a DL model for classifying the presence and absence of plateau iris from AS-OCT images. The two DL models mentioned previously were developed and validated on datasets of AS-OCT images with the aim of applying the models to AS-OCT images. In the present study, we developed a DL model to predict the presence of plateau iris based on a dataset of AS-OCT images with information and labels transferred from a dataset of paired UBM images. We validated the model on a test set of new AS-OCT images with ground truth from UBM as the reference standard.

This approach of "label transfer" for DL has been used in a few recent studies of glaucoma. In a study by Medeiros et al.,[17] paired data of color photographs of ONH and RNFL thickness from OCT were used to train a DL model to be able to predict RNFL thickness from assessment by color photographs only of ONH. From a dataset of 32,820 pairs of the data, with 80% for training and 20% for testing, this DL model demonstrated a strong correlation between predicted and observed RNFL thickness, and it showed AUC of 0.95 for discrimination between healthy eyes and those with glaucomatous damage. The same model also demonstrated better performance when compared with human graders (absolute correlation with standard automated perimetry [SAP] mean deviation at the rho value of 0.54 vs. 0.48, and partial AUC of 0.529 vs. 0.411) to discriminate between glaucomatous optic neuropathy and ONH of healthy subjects.

In the present study, we did not use only labels transferred from UBM to train our DL prediction model (ResNet50); we also utilized a "style transfer" or image-to-image translation, which is another DL approach (CycleGAN), for augmentation of AS-OCT images, using UBM images as part of the training. Interestingly, we found that without the style transfer - with only the label transfer - our model did not perform well in predicting the presence or absence of plateau iris (AUC = 0.67). It was when the prediction model included images with style transfer for training that it achieved significantly better performance (AUC = 0.95). This was also reflected in training when performances of the model on images from each augmentation function were better when the prediction model that included images with the style transfer was used. As the structures behind the iris are poorly imaged by the AS-OCT due to light attenuation and limited penetration, DL may not directly use this data for prediction; however, our model was able to make predictions with acceptable accuracy. This may be viewed as a limitation, as described in the Black-box in DL, and further validation of our models in new datasets is required to support this.

The same approach of style transfer has been applied to improve visualization of medical images in the past; for example, in radiology, visualization of skulls on magnetic resonance images (MRIs) has been enhanced by style transfer of corresponding computed tomography (CT) scan images.[25] In ophthalmology, style transfer has been used to improve resolution and visualization of blood vessels in fundus images using another set of good resolution fundus images.[26] In another example, styles of normal OCT images were transferred to contents of abnormal OCT images using another approach of style transfer (AnoGAN) to detect abnormalities, such as intraretinal or subretinal fluid, in order to create a marker for disease progression on OCT.[27] This DL approach should be explored further for its potential role in imaging studies in ophthalmology.

There have been some previous studies of manual grading of AS-OCT images to detect plateau iris.[28–31] This condition was subjectively described as peripheral iris rising up from the iris root, in apposition to the anterior chamber angle, and turning flat centrally while the anterior chamber depth appeared to be normal; however, these studies had no data from dynamic gonioscopy or UBM demonstrating the position of the ciliary process to support the presence of plateau iris. In addition, there were no reports on diagnostic performance, such as sensitivity, specificity, and accuracy for the detection of plateau iris with the manual grading of AS-OCT images in these studies.

There are limited numbers of studies of plateau iris based on UBM in the literature. In a study in the United States, it was found to be the most common cause of angle-closure glaucoma (52%) in patients younger than 40 years old.[32] In other studies in Asia, it was responsible for about one-third of patients with PACD.[4,5,33,34] The prevalence of plateau iris in PACD in Chinese populations has been reported to be 44.7%.[35] A recent study found a similar prevalence of plateau iris in PACD in Caucasians and Asians.[36] In this study, also based on UBM, we found plateau iris in 38.6% of quadrants of the eyes of the patients with PACD suggesting that this disease may not be uncommon.

There could be many applications of the DL model developed in this study to assist clinicians in making decisions when plateau iris is found in PACD, particularly when UBM is not readily available. First, in patients with appositional close angle post-LPI, plateau iris should be ruled out. Second, in patients with asymptomatic plateau iris, prophylactic laser iridoplasty may be performed to keep the anterior chamber angle open. Third, in patients with PACD before and after glaucoma filtering surgery, the detection of plateau iris could also help clinicians to make proper judgment and management in order to avoid serious complications after surgery. In this regard, a report by Prata et al. showed that in patients with preoperative plateau iris configuration identified by UBM, 85% (11/13 eyes) developed malignant glaucoma after trabeculectomy.[37,38]

One of the limitations of this study was the lack of validation of the model in a new dataset of AS-OCT consisting of patients with PACD. It is still possible that the results of our study are overfit with a new dataset. In future plans to train and validate this model, datasets used should include those from different clinical settings, populations, and ethnicities. Although we believe that training and testing using images from two different UBM devices in this study might have had no effect on model performance, this point should be addressed in another study. Similarly, training and testing on datasets from different AS-OCT devices and technologies, such as spectral-domain or swept-sourced, may also be required.

The relatively small sample size was another limitation, although we believe that our model should perform better with a greater number of images and datasets of paired AS-OCT and UBM. Whereas other DL models in ophthalmology can take advantage of easily accessible open-sourced, online datasets, such as color retinal photographs, the open-sourced dataset of AS-OCT for PACD is unfortunately not readily available. The labeling of the data in our study was carried out by a single rater, and this might be considered another limitation.

In summary, we developed a DL model to be applied with AS-OCT to predict the presence or absence of plateau iris. The model was capable of making predictions with high diagnostic performance at both image and patient levels. This model could potentially assist clinicians for management of the disease in order to avoid its irreversible consequences.

Acknowledgments

Supported by a Rajavithi Hospital research fund, grant number 030/2563, Thammasat University's research fund, Center of Excellence in Intelligent Informatics, Speech and Language Technology and Service Innovation (CILS), and the Intelligent Informatics and Service Innovation (IISI) Research Center, Thailand Research Fund grant number RTA6080013, and the TRF Research Team Promotion Grant (RTA), grant number RTA6280015. The authors would like to thank John Flanagan, MA, for proofreading the manuscript.

The authors alone are responsible for the content and writing of the paper.

Disclosure: **B. Wanichwecharungruang,** None; **N. Kaothanthong,** None; **W. Pattanapongpaiboon**, None; **P. Chantangphol**, None; **K. Seresirikachorn,** None; **C. Srisuwanporn,** None; **N. Parivisutt,** None; **A. Grzybowski,** None; **T. Theeramunkong,** None; **P. Ruamviboonsuk,** None

References

1. Wand M, Grant WM, Simmons RJ, Hutchinson BT. Plateau iris syndrome. *Trans Am Acad Ophthalmol Otolaryngol*. 1977;83:122–130.
2. Ritch R, Lowe RF. Angle-closure glaucoma: mechanisms and epidemiology. In: Ritch R, Shields MB, Krupin T, eds. *The glaucomas*. St. Louis, MO: Mosby, 1996; v. 2nd.
3. Pavlin CJ, Ritch R, Foster FS. Ultrasound biomicroscopy in plateau iris syndrome. *Am J Ophthalmol*. 1992;113(4):390–395.
4. Kumar RS, Tantisevi V, Wong MH, et al. Plateau iris in Asian subjects with primary angle closure glaucoma. *Arch Ophthalmol*. 2009;127(10):1269–1272.
5. Kumar RS, Baskaran M, Chew PT, et al. Prevalence of plateau iris in primary angle closure suspects an ultrasound biomicroscopy study. *Ophthalmology*. 2008;115(3):430–434.
6. Radhakrishnan S, Rollins AM, Roth JE, et al. Real-time optical coherence tomography of the anterior segment at 1310 nm. *Arch Ophthalmol*. 2001;119:1179–1185.
7. Dorairaj S, Tsai JC, Grippo TM. Changing trends of imaging in angle closure evaluation. *ISRN Ophthalmol*. 2012;2012:597124.
8. Parc C, Laloum J, Berges O. Comparison of optical coherence tomography and ultrasound biomicroscopy for detection of plateau iris. *J Fr Ophtalmol*. 2010;33(4):266–273.
9. Shen D, Wu G, Suk H-I. Deep learning in medical image analysis. *Ann Rev Biomed Engineer*. 2017;19(1):221–248.
10. Ting DSW, Peng L, Varadarajan AV, et al. Deep learning in ophthalmology: the technical and clinical considerations. *Prog Retin Eye Res*. 2019;72:100759.
11. Asaoka R, Murata H, Iwase A, Araie M. Detecting preperimetric glaucoma with standard automated perimetry using a deep learning classifier. *Ophthalmology*. 2016;123(9):1974–1980.
12. Lee CS, Baughman DM, Lee AY. Deep learning is effective for classifying normal versus age-related macular degeneration OCT images. *Ophthalmol Retina*. 2017;1(4):322–327.
13. Ting DSW, Cheung CY, Lim G, et al. Development and validation of a deep learning system for diabetic retinopathy and related eye diseases using retinal images from multiethnic populations with diabetes. *JAMA*. 2017;318(22):2211–2223.
14. Christopher M, Belghith A, Bowd C, et al. Performance of deep learning architectures and transfer learning for detecting glaucomatous optic neuropathy in fundus photographs. *Sci Rep*. 2018;8(1):16685.
15. Grzybowski A, Brona P, Lim G, et al. Artificial intelligence for diabetic retinopathy screening: a review. *Eye*. 2020;34(3):451–460.
16. Ruamviboonsuk P, Krause J, Chotcomwongse P, et al. Deep learning versus human graders for classifying diabetic retinopathy severity in a nationwide screening program. *NPJ Digit Med*. 2019;10(2):25.
17. Medeiros FA, Jammal AA, Thompson AC. From Machine to Machine: An OCT-Trained Deep Learning Algorithm for Objective Quantification of Glaucomatous Damage in Fundus Photographs. *Ophthalmology*. 2019;126(4):513–521.
18. Foster PJ, Buhrmann R, Quigley HA, Johnson GJ. The definition and classification of glaucoma in prevalence surveys. *BrJ Ophthalmol*. 2002;86(2):238–242.
19. Ritch R. Plateau iris is caused by abnormally positioned ciliary body. *J Glaucoma*. 1992;1:23–26.
20. Bengio Y, Courville A, Vincent P. Representation Learning: A Review and New Perspectives. *IEEE Transactions on Pattern Analysis and Machine Intelligence*. 2013;35(8):1798–1828.
21. Gatys LA, Ecker AS, Bethge M. Image style transfer using convolutional neural networks. In *Proceedings of the IEEE Conference on Computer Vision and Pattern Recognition (CVPR)*, Las Vegas, NV, 2016. pp. 2414–2423.
22. Zhu J-Y, Park T, Isola P, Efros AA. Unpaired image-to-image translation using cycle-consistent adversarial networks. *2017 IEEE International Conference on Computer Vision (ICCV)*, Venice, 2017. pp. 2242–2251.
23. Fu H, Baskaran M, Xu Y, et al. A deep learning system for automated angle-closure detection in anterior segment optical coherence tomography images. *Am J Ophthalmol*. 2019;203:37–45.
24. Xu BY, Chiang M, Chaudhary S, et al. Deep learning classifiers for automated detection of gonio-

scopic angle closure based on anterior segment OCT images. *Am J Ophthalmol*. 2019;208:273–280.
25. Wolterink JM, Dinkla AM, Savenije MHF, et al. Deep MR to CT synthesis using unpaired data. arXiv e-prints 2017. Available at: https://arxiv.org/abs/1708.01155.
26. Mahapatra D, Bozorgtabar B. Retinal vasculature segmentation using local saliency maps and generative adversarial networks for image super resolution. arXiv e-prints 2017. Available at: https://arxiv.org/abs/1710.04783v1.
27. Schlegl T, Seeböck P, Waldstein SM, et al. Unsupervised anomaly detection with generative adversarial networks to guide marker discovery. In: Niethammer M, Styner M, Aylward S, et al., eds. Information Processing in Medical Imaging. Cham, Switzerland: Springer International Publishing; 2017.
28. Shabana N, Aquino MC, See J, et al. Quantitative evaluation of anterior chamber parameters using anterior segment optical coherence tomography in primary angle closure mechanisms. *Clin Exp Ophthalmol*. 2012;40(8):792–801.
29. Kwon J, Sung KR, Han S. Long-term changes in anterior segment characteristics of eyes with different primary angle-closure mechanisms. *Am J Ophthalmol*. 2018;191:54–63.
30. Moghimi S, Zandvakil N, Vahedian Z, et al. Acute angle closure: qualitative and quantitative evaluation of the anterior segment using anterior segment optical coherence tomography. *Clin Exp Ophthalmol*. 2014;42(7):615–622.
31. Zhang Y, Li SZ, Li L, et al. Quantitative analysis of iris changes following mydriasis in subjects with different mechanisms of angle closure. *Invest Ophthalmol Vis Sci*. 2015;56(1):563–570.
32. Ritch R, Chang BM, Liebmann JM. Angle closure in younger patients. *Ophthalmology*. 2003;110(10):1880–1889.
33. Kumar G, Bali SJ, Panda A, et al. Prevalence of plateau iris configuration in primary angle closure glaucoma using ultrasound biomicroscopy in the Indian population. *Indian J Ophthalmol*. 2012;60(3):175–178.
34. Mansoori T, Sarvepally VK, Balakrishna N. Plateau iris in primary angle closure glaucoma: an ultrasound biomicroscopy study. *J Glaucoma*. 2015;25(2):e82–e86.
35. Yan YJ, Wu LL, Wang X, Xiao GG. Appositional angle closure in Chinese with primary angle closure and primary angle closure glaucoma after laser peripheral iridotomy. *Invest Ophthalmol Vis Sci*. 2014;55(12):8506–8512.
36. Li Y, Wang YE, Huang G, et al. Prevalence and characteristics of plateau iris configuration among American Caucasian, American Chinese and mainland Chinese subjects. *Br J Ophthalmol*. 2014;98(4):474–478.
37. Prata TS, Dorairaj S, De Moraes CG, et al. Is preoperative ciliary body and iris anatomical configuration a predictor of malignant glaucoma development? *Clin Experiment Ophthalmol*. 2013;41(6):541–545.
38. Grzybowski A, Kanclerz P. Acute and chronic fluid misdirection syndrome: pathophysiology and treatment. *Graefes Arch Clin Exp Ophthalmol*. 2018;256(1):135–154.